

HIV-1 Nef promotes infection by excluding SERINC5 from virion incorporation

Annachiara Rosa^{1*}, Ajit Chande^{1*}, Serena Ziglio^{1*}, Veronica De Sanctis², Roberto Bertorelli², Shih Lin Goh³, Sean M. McCauley³, Anetta Nowosielska³, Stylianos E. Antonarakis^{4,5}, Jeremy Luban³, Federico Andrea Santoni⁴ & Massimo Pizzato¹

HIV-1 Nef, a protein important for the development of AIDS, has well-characterized effects on host membrane trafficking and receptor downregulation. By an unidentified mechanism, Nef increases the intrinsic infectivity of HIV-1 virions in a host-cell-dependent manner. Here we identify the host transmembrane protein SERINC5, and to a lesser extent SERINC3, as a potent inhibitor of HIV-1 particle infectivity that is counteracted by Nef. SERINC5 localizes to the plasma membrane, where it is efficiently incorporated into budding HIV-1 virions and impairs subsequent virion penetration of susceptible target cells. Nef redirects SERINC5 to a Rab7-positive endosomal compartment and thereby excludes it from HIV-1 particles. The ability to counteract SERINC5 was conserved in Nef encoded by diverse primate immunodeficiency viruses, as well as in the structurally unrelated glycosylated Gag from murine leukaemia virus. These examples of functional conservation and convergent evolution emphasize the fundamental importance of SERINC5 as a potent anti-retroviral factor.

Nef is a 27–32-kilodalton (kDa) protein expressed uniquely by primate lentiviruses that has a fundamental role in virus replication and the development of AIDS^{1–3}. It is a multifunctional factor that performs a plethora of activities within the cell, among which is the ability to downregulate crucial cell surface molecules (including CD4, MHC-I and T-cell receptor) via interaction with vesicular trafficking machinery⁴. Other activities of Nef include the ability to alter the activation state of T cells and macrophages^{5–8} and to perturb the actin cytoskeleton⁹ by engaging with cellular kinases. These relatively well-characterized activities, however, do not explain another function of Nef that was reported 20 years ago¹⁰, that is, its ability to enhance the infectivity of the virion. The latter activity seems to be important for HIV-1 pathogenesis because it is phylogenetically conserved among widely divergent primate lentiviruses¹¹ and maintained under strong selective pressure during disease progression¹². Such enhancement of virion infectivity depends on *nef* being expressed from within virus-producing cells¹³, but it is manifest at an early stage in the subsequent infection of susceptible target cells^{13–15}, indicating a yet unknown modification of progeny virus particles.

Although Nef is unique to HIV and SIV, glycosylated Gag from an unrelated gammaretrovirus (Moloney murine leukaemia (MLV)) fully substitutes for the activity of Nef on HIV-1 infectivity¹⁶. Despite the lack of any sequence homology, Nef and glycosylated Gag share a remarkable functional similarity, as they both require host cell endocytosis machinery to boost virion infectivity¹⁷. A Nef-like activity promoting retrovirus infectivity has therefore arisen by convergent evolution within an unrelated family of retroviruses. However, the molecular mechanism underlying the requirement of Nef and glycosylated Gag for retrovirus infectivity has so far remained elusive.

Nef counteracts a retrovirus inhibitor

We investigated to what extent the Nef requirement for virion infectivity is producer cell-type dependent, by comparing the infectivity of wild-type HIV-1 to its Nef-defective counterpart produced from 31 different

human cell lines (Fig. 1a and Extended Data Table 1). Varying with the producer cell type, the effect of Nef ranged from 2- to 40-fold, arguing in favour of the presence of a cellular inhibitor of HIV-1 counteracted by Nef. We then investigated whether this Nef responsiveness is a dominant feature in producer cells by generating Nef-positive and Nef-negative HIV-1 virions from heterokaryons derived from cell lines with opposite Nef-responsiveness (Fig. 1b). When lymphoid cells (high Nef responsive) were fused with fibrosarcoma cells (low Nef responsive), HIV-1 produced by heterokaryons displayed relatively high dependence on Nef (Fig. 1c), indicating the presence of a transdominant cellular inhibitor of HIV-1 infectivity counteracted by Nef.

To identify such a putative host factor, the global transcriptome of high and low Nef-responsive cells was examined to pinpoint differentially expressed genes that correlate with Nef responsiveness. Transcriptomes from seven highly Nef-responsive cell lines (Nef effect ranging from 10- to 40-fold) and eight low Nef-responsive cell lines (Nef effect lower than fourfold) were subjected to RNA-sequencing (RNA-seq). On the basis of correlation analysis, SERINC5 emerged as the gene whose expression correlated best with the requirement of Nef for HIV-1 infectivity (Fig. 1d).

SERINC5 inhibits HIV-1 and MLV

To validate functionally the effect on virion infectivity, the SERINC5 genomic sequence was disrupted in the cell line with the highest Nef responsiveness (Jurkat TAg or JTAg) using a clustered regularly interspaced short palindromic repeat (CRISPR)-Cas9 lentiviral vector (Extended Data Fig. 1a). SERINC5 knockout cells produced a 20–30-fold increase in the infectivity of the Nef-defective HIV-1, whereas the Nef-positive virus was only affected 2–3-fold, thus reducing the Nef effect from 50- to 3-fold (Fig. 2a, b). This result was reproduced targeting three different regions of the SERINC5 gene (Extended Data Fig. 1b). When haemagglutinin (HA)-tagged SERINC5 was expressed from a complementary DNA non-targetable by the CRISPR-Cas9 vector, the high Nef-dependent phenotype was

¹University of Trento, Centre for Integrative Biology, 38123 Trento, Italy. ²University of Trento, Laboratory of Biomolecular Sequence and Structure Analysis for Health, NGS facility, 38123 Trento, Italy. ³University of Massachusetts Medical School, Program in Molecular Medicine, Worcester, Massachusetts 01605, USA. ⁴University of Geneva, Department of Genetic Medicine and Development, Geneva 1211, Switzerland. ⁵iGE3 Institute of Genetics and Genomics of Geneva, Geneva 1211, Switzerland.

*These authors contributed equally to this work.

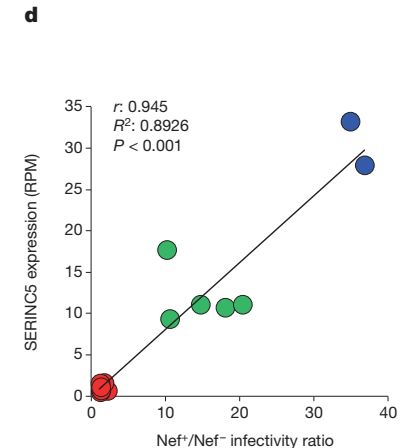
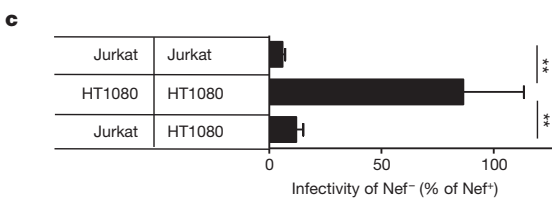
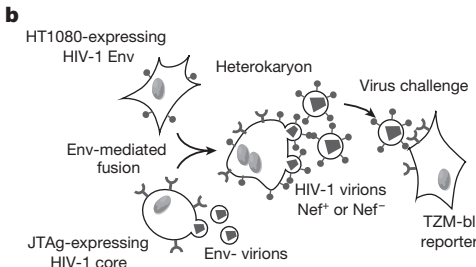
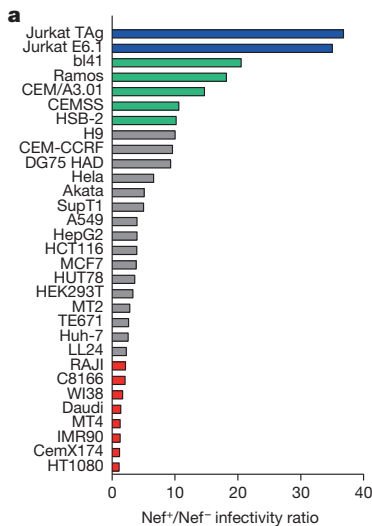


Figure 1 | Nef counteracts an HIV-1 inhibitor. **a**, Ratio of the infectivity of NL4-3 and NL4-3^{Nef-} produced from the indicated cell lines and measured on TZM-bl reporter cells. **b**, The schematic of the heterokaryon assay. **c**, Infectivity of HIV-1 derived from heterokaryons generated by the indicated cell lines ($n = 3$, mean \pm s.d., unpaired t -test, ** $P < 0.01$).

d, Correlation of SERINC5 expression in producer cells and Nef requirement for infectivity. Colours in **a** and **d** represent the same cell lines. Trendline indicates linear regression. (Pearson correlation, two-tailed, $P < 0.0001$). RPM, reads per million.

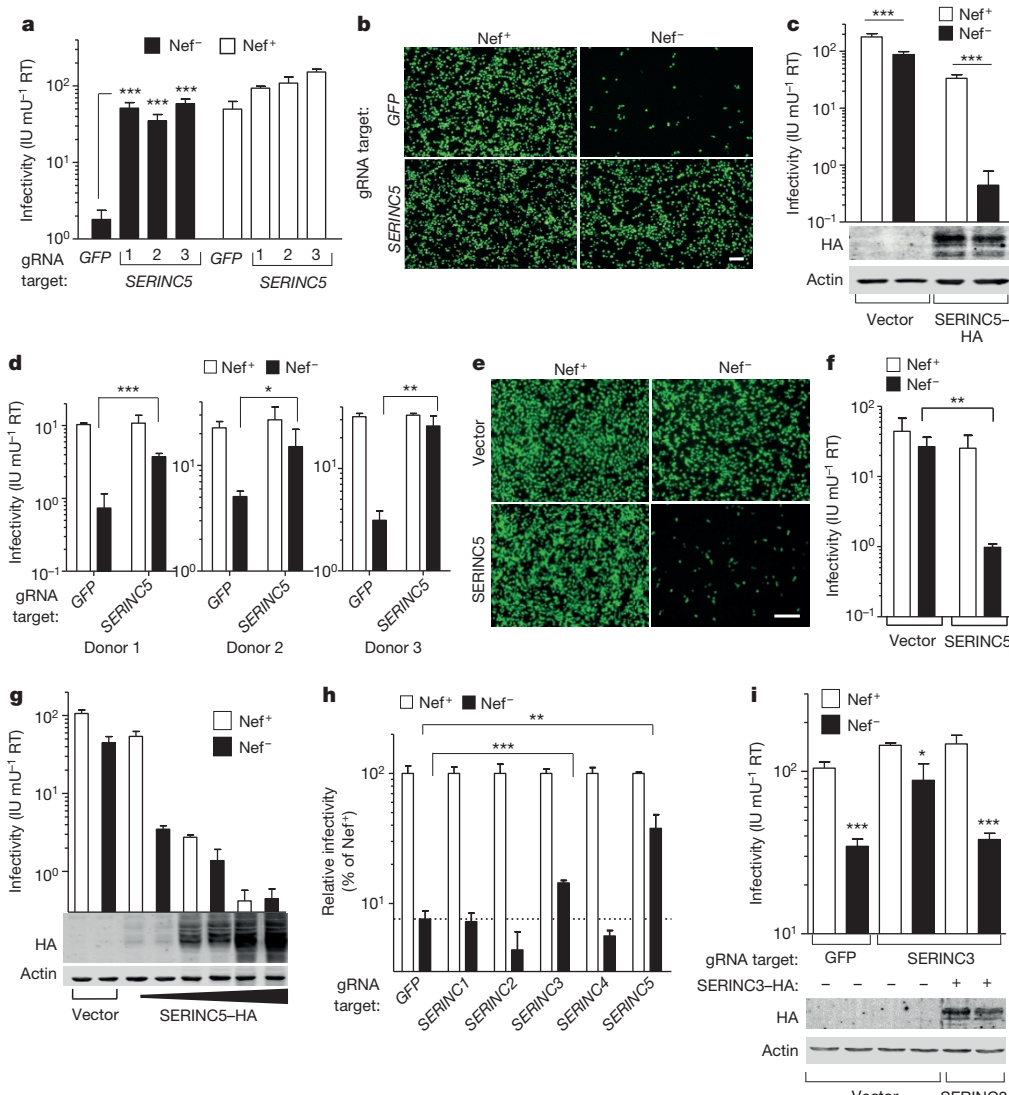


Figure 2 | SERINC5 and SERINC3 inhibit HIV-1.

a, Infectivity of HIV-1 from cells stably transduced with lentiCRISPR ($n = 4$). gRNA, guide RNA; RT, reverse transcriptase. **b**, Fluorescence microscopy of reporter cells from **a**. **c**, Infectivity of HIV-1 from JTAg *SERINC5*^{-/-} and immunoblotting of producer cells. **d**, Infectivity of HIV-1 from PBMC, co-transfected with CRISPR-Cas9 vectors ($n = 3$, one experiment performed per donor). **e–g**, Infectivity of HIV-1 from HEK293T expressing SERINC5-HA. Reporter cells infected with HIV-1 from HEK293T expressing SERINC5-HA ($n = 4$). **h**, **i**, Infectivity of HIV-1 produced from JTAg (**h**) and JTAg *SERINC5*^{-/-} (**i**) transfected with CRISPR-Cas9 vectors targeting the indicated SERINC genes ($n = 4$). In **i**, immunodetection of SERINC3-HA in producer cells. Mean \pm s.d., unpaired two-tailed t -test, * $P < 0.05$, ** $P < 0.01$, *** $P < 0.001$. Scale bars, 100 μ m.

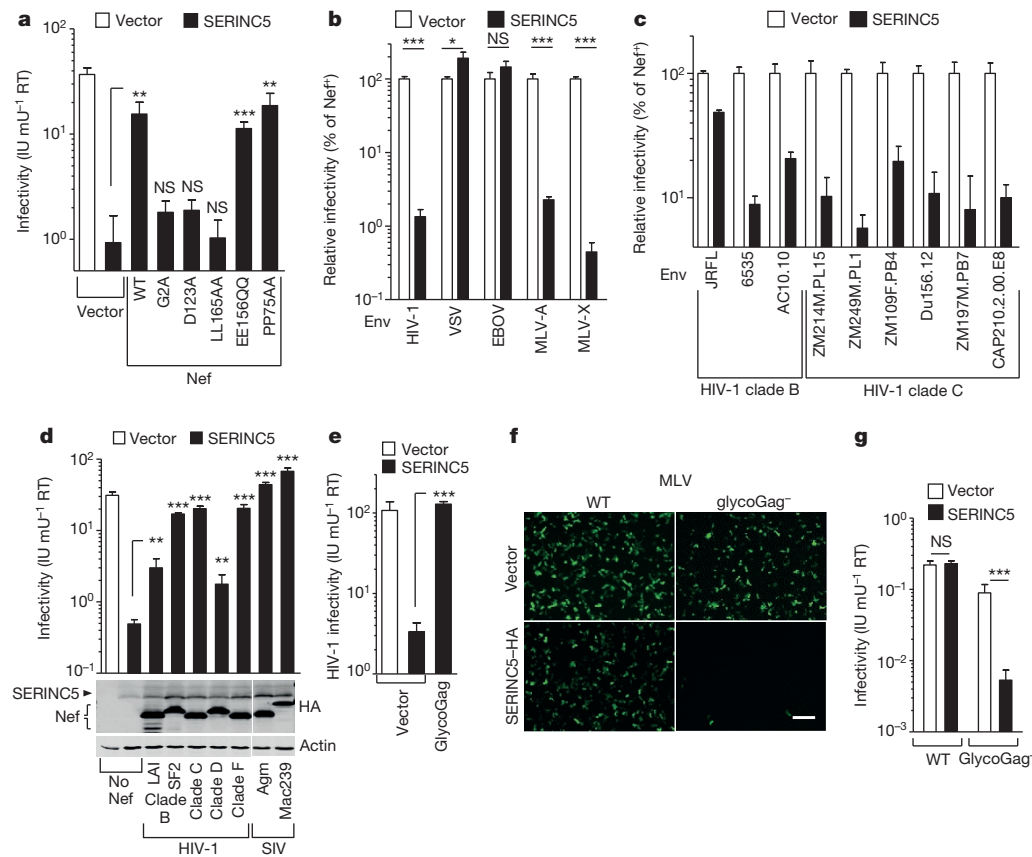


Figure 3 | Determinants of Nef activity against SERINC5 and conservation across different retroviruses. **a**, The ability of Nef mutants to counteract SERINC5 inhibition of HIV-1 infectivity ($n = 4$). **b, c**, Susceptibility of viral pseudotypes to inhibition of infectivity by SERINC5 ($n = 4$). **d, e**, Counteraction of SERINC5 by nef alleles and immunoblot from producer cells (**d**) and glycoGag (**e**) on HIV-1. **f, g**, Infectivity of wild-type and glycoGag-defective MLV from HEK293T expressing SERINC5 ($n = 4$). Mean \pm s.d., unpaired two-tailed *t*-test, * $P < 0.05$, ** $P < 0.01$, *** $P < 0.001$; NS, not significant. Scale bar, 100 μ m.

restored (Fig. 2c), and the infectivity of the Nef-defective HIV-1 was reduced 197-fold versus a fivefold only reduction of the Nef-positive counterpart. SERINC5 was found to be expressed in primary blood cells from three different donors to a level comparable to that observed in Jurkat cells (Extended Data Fig. 1c). Accordingly, CRISPR-Cas9 vector-mediated SERINC5 knockout cells increased specifically the infectivity of Nef-defective HIV-1 produced in cultured peripheral blood mononuclear cells (PBMC) derived from three different individuals (Fig. 2d), demonstrating that SERINC5 inhibits HIV-1 produced in primary human blood cells.

Ectopic expression of SERINC5 in cells with minimal Nef-dependence (Fig. 2e, f and Extended Data Fig. 1d), resulted in a 10–40-fold selective inhibition of Nef-defective HIV-1. SERINC5 is therefore not only required, but also sufficient to inhibit HIV-1 infection and to confer Nef responsiveness. While inhibition of HIV-1 infection by SERINC5 is dose-dependent (Fig. 2g), the ability of Nef to preserve the infectivity of the virus particle is abolished with increasing expression of SERINC5, suggesting that the ability of Nef to counteract SERINC5 is saturable (Fig. 2g). At the highest SERINC5 expression level, virion infectivity was reduced 256-fold, regardless of Nef expression.

SERINC5 belongs to a unique gene family present in all eukaryotes and contains 10 putative transmembrane helices^{18,19}. While it was suggested that SERINC proteins mediate incorporation of serine into membrane lipids²⁰, their function is unknown. The five members of the human SERINC family share more than 17% amino acid identity and a similarly predicted membrane topology. We observed that virus produced in JTAg SERINC5^{-/-} cells retains a 2–3-fold responsiveness to Nef (Fig. 2a). Our transcriptome analysis indicated that JTAg cells express other SERINC genes in addition to SERINC5 (Extended Data Fig. 1e). We therefore explored the possibility that other SERINC family members have anti-HIV-1 activity by knocking out the five SERINC genes individually. Targeting SERINC3 in JTAg SERINC5^{-/-} cells resulted in a 2–3-fold rescue of Nef-defective virus

infectivity (Fig. 2i), thus further reducing the residual Nef responsiveness to 1.6-fold (Fig. 2i). Ectopic expression of SERINC3 resulted in threefold inhibition of Nef-defective HIV-1 (Fig. 2i), confirming that SERINC3 can also inhibit HIV-1 infectivity.

The Nef activity against SERINC5

The effect of Nef on infectivity requires Nef myristylation and interaction with clathrin-mediated endocytosis^{21,22} (AP2 and dynamin2). Accordingly, the ability to counteract SERINC5 was impaired by nef mutations that abolish Nef amino-terminal myristylation (G2A), disrupt a di-leucine-based sorting signal (LL165AA) necessary for AP2 interaction²¹, or prevent binding to dynamin 2 (D123A, Fig. 3a)²². By contrast, mutations abrogating either a proline-rich SH3 binding domain (PP75AA)²³, or di-acidic motif required for CD4 downregulation (EE156QQ)²⁴, do not affect the ability to counteract SERINC5 (Fig. 3a). The molecular features of Nef already known to be crucial for the effect on infectivity are therefore required for counteracting SERINC5.

It has been reported that the effect of Nef on infectivity depends on the nature of the envelope glycoprotein^{16,25–29}. Accordingly, pseudotyping HIV-1 with vesicular stomatitis virus G protein (VSV-G) and with the Ebola virus glycoprotein (EBOV GP), but not with MLV-A nor MLV-X Env, makes HIV-1 resistant to SERINC5 (Fig. 3b). The magnitude of the effect of Nef on infectivity was also reported to vary when HIV-1 is pseudotyped with envelope glycoproteins derived from different HIV-1 isolates^{30,31}. Accordingly, virions carrying Env derived from a panel of HIV-1 primary isolates were variably affected by SERINC5 (Fig. 3c), indicating that naturally occurring isolates are inhibited by the host factor to different extents.

The activity of Nef on infectivity is highly conserved among primate lentiviruses¹¹. We therefore tested whether the ability to counteract SERINC5 is shared among nef alleles. Nef proteins derived from subtypes B, C, D and F clinical isolates could counteract ectopically

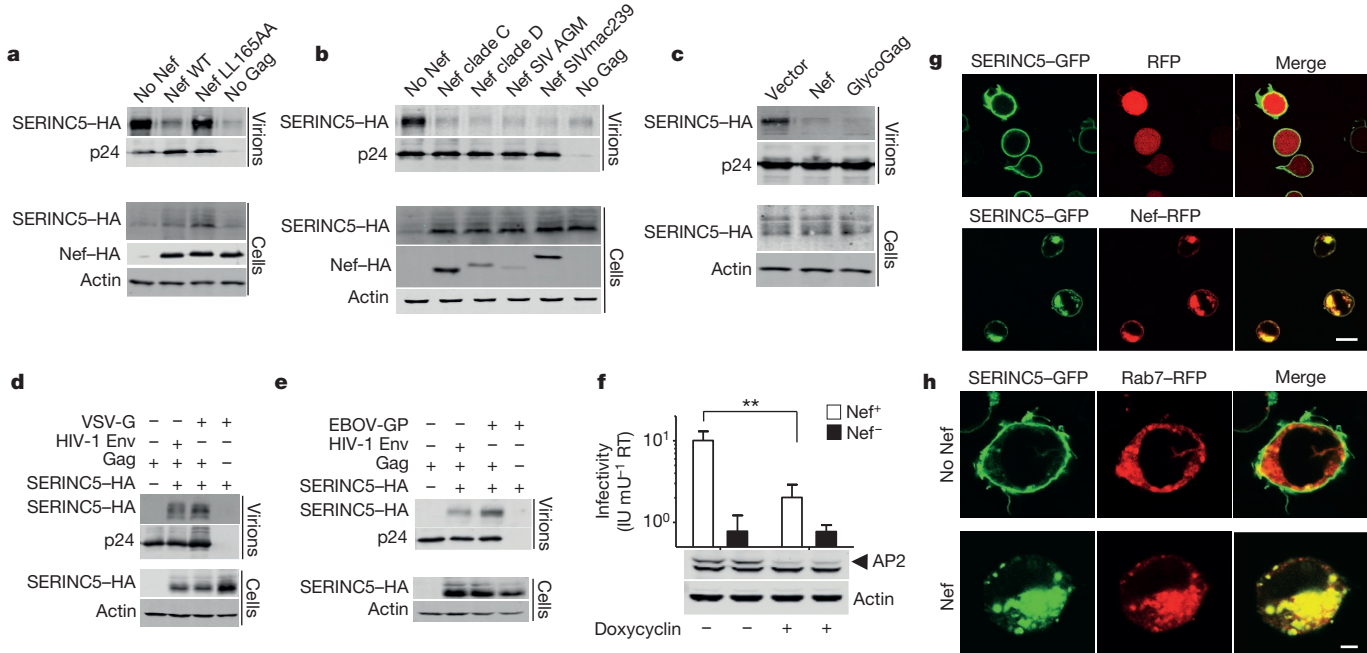


Figure 4 | Nef and glycoGag promote relocation of SERINC5 to an endosomal compartment and prevent its incorporation into virions.

a–e, Immunoblots on viral particles and corresponding cell lysates from *nef*-defective NL4-3 complemented with plasmids encoding Nef proteins as indicated (**a** and **b**), MLV glycoGag (**c**), VSV-G (**d**) EBOV-GP (**e**) and a vector expressing SERINC5-HA. **f**, Infectivity of HIV-1 from HEK293T cells stably

expressed SERINC5-HA with a potency 5–10-fold higher than that observed with Nef derived from a laboratory adapted strain (HIV-1_{LAI}, Fig. 3d). Similarly, Nef from two divergent SIV lineages (SIVmac239 and SIVagm) also counteracted SERINC5 with tenfold higher efficacy than HIV-1_{LAI} (Fig. 3d). The ability to counteract SERINC5 is therefore a prominent feature of Nef, conserved across different primate lentivirus species.

We next tested whether SERINC5 can target retroviruses other than lentiviruses. We have shown that glycosylated Gag (glycoGag) from MLV is capable of rescuing the infectivity of Nef-defective HIV-1 (ref. 16), despite sharing no sequence homology with Nef. Indeed, glycoGag efficiently rescues the infectivity of HIV-1 (Fig. 3e) by counteracting SERINC5, suggesting that SERINC5 has an important role also in the context of infection with gammaretroviruses. Accordingly, SERINC5 expression in producer cells potently inhibited infectivity of MLV only in the absence of glycoGag (Fig. 3f, g). Therefore, while SERINC5 targets divergent retroviruses, factors capable of overcoming its inhibitory activity on infectivity have evolved independently.

Incorporation of SERINC5 into virions

The ability of SERINC5 to be incorporated into the lipid envelope of HIV-1 virions was tested next. HIV-1 was produced in JTAG *SERINC5*^{-/-} expressing SERINC5-HA. Despite being barely detectable in cells in the absence of Nef, SERINC5-HA was readily visualized in Nef-defective virions and was largely excluded from virions generated in the presence of Nef (Fig. 4a) but not in the presence of the Nef mutant lacking the AP2 binding site (LL165AA, Fig. 4a). The ability to prevent virion incorporation of SERINC5 was readily observed with Nef alleles from HIV-1 and SIV (Fig. 4b) and with MLV glycoGag (Fig. 4c), suggesting that association with virions is crucial for the effect on infectivity and is tightly controlled by both primate lentiviral and gammaretroviral factors. The effect of Nef on SERINC5 association with virions did not alter the amount of incorporated Env (Extended Data Fig. 2a), in line with previous

expressing a doxycycline-inducible shRNA targeting AP2 and transfected with PBJ6-SERINC5. Western blot: AP2 in cell lysates derived from producer cells (mean \pm s.d., $n = 4$ unpaired two-tailed *t*-test, ** $P < 0.01$, experiment replicated twice). **g, h**, Confocal microscopy of JTAG cells transfected to express SERINC5-GFP with RFP, Nef-RFP (**g**) or Rab7-RFP (**h**). Scale bars, 10 μm (**g**) and 2 μm (**h**).

observations that failed to observe any effect of Nef on virion Env abundance^{16,25,31}. By contrast, the amount of SERINC5 incorporated into HIV particles was not reduced by VSV-G (Fig. 4d) nor by EBOV GP (Fig. 4e), despite the infectivity of VSV-G and EBOV GP pseudotypes being resistant to the host factor (Fig. 3b). Therefore, while Nef and glycoGag seem to counteract SERINC5 by preventing its incorporation into virions, VSV-G and EBOV GP must antagonize its effect by a different mechanism.

The ability of Nef to counteract SERINC5 was significantly reduced by silencing AP2 (Fig. 4f), confirming the crucial involvement of clathrin-dependent intravesicular trafficking. Using immunofluorescence microscopy, green fluorescent protein (GFP)-tagged SERINC5 (Fig. 4g) was observed to localize almost exclusively to the plasma membrane. By contrast, the expression of HIV-1 Nef caused SERINC5 to relocate together with Nef into perinuclear vesicles identified as late endosomes (RAB7-positive, Fig. 4h). SERINC5 was similarly efficiently retargeted into perinuclear vesicles by SIV Nef and by MLV glycoGag (Extended Data Fig. 2b), indicating a common ability of the retroviral factors to relocate SERINC5, which is removed from the plasma membrane, and prevented from accessing nascent virions.

The anti-HIV-1 activity of SERINC5

Which step of the HIV-1 life cycle is blocked by SERINC5 was investigated next. HIV-1 produced in the presence of SERINC5-HA failed to accumulate products of reverse transcription in target cells, confirming previous reports that in the absence of Nef the infection process is halted at an early stage of the HIV-1 life cycle (Fig. 5a). Whether Nef affects fusion between the virion particle and the target cell membrane has remained questionable^{25,32–37}. We therefore developed a novel protein transduction assay in which the bacteriophage Cre recombinase fused to a nuclear localization signal flanked by HIV-1 protease cleavage sites (Fig. 5b) is packaged as part of the Gag polyprotein into HIV-1 particles (Extended Data Fig. 3a). Cre, delivered into the cell after fusion, activates expression of a reporter

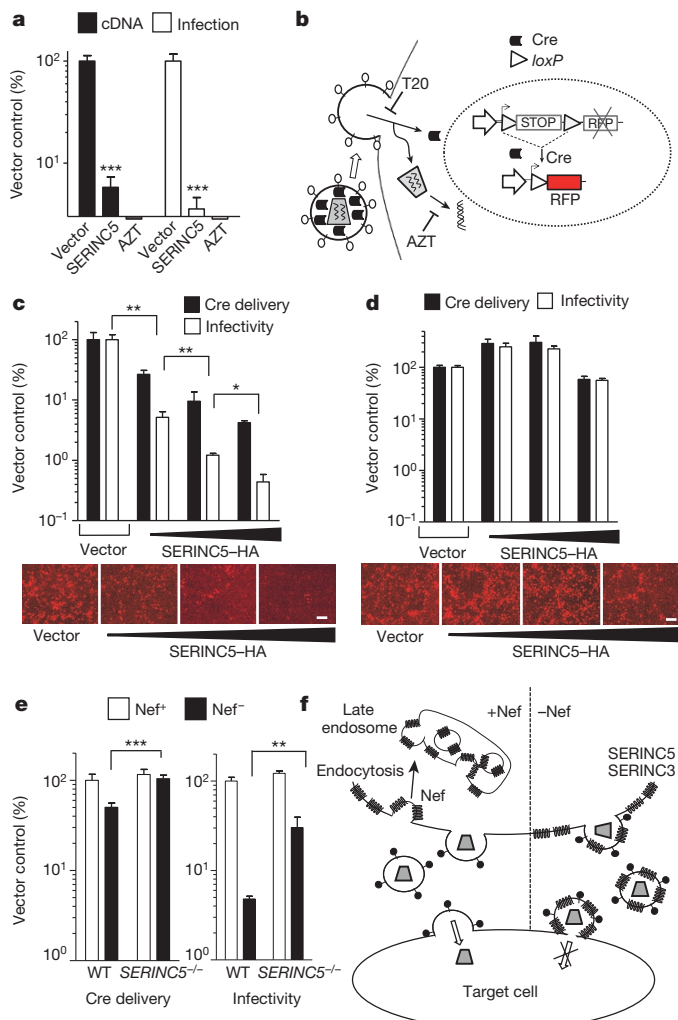


Figure 5 | SERINC5 inhibits an early step of virus infection. **a**, Effect of SERINC5 on the generation of HIV-1 late reverse transcription products ($n = 3$; experiments replicated twice) and the corresponding effect on infectivity. **b**, Schematic of the nlsCre delivery assay. **c, d**, Effect of SERINC5 on Cre-delivery by HIV-1 (c) and HIV-1 pseudotyped with VSV-G (d). **e**, Cre delivery and infectivity by HIV-1-derived from JTAG or JTAG *SERINC5*^{-/-}. **f**, Schematic showing the activity of SERINC5 on HIV-1 infectivity and the counteracting mechanism by Nef. Mean \pm s.d., $n = 4$, unpaired two-tailed *t*-test, **P* < 0.05, ***P* < 0.01, ****P* < 0.001. Scale bars, 100 μ m.

gene (nlsRFP) following *loxP* recombination. Confirming the ability to detect cytoplasmic delivery of Cre independently of productive infection, Cre-mediated reporter activation was not blocked by the reverse transcriptase inhibitor azidothymidine (AZT) but was blocked by the fusion inhibitor T20 (Extended Data Fig. 3b).

Increasing expression of SERINC5 in producer cells did not affect the amount of Cre associated with virions (Extended Data Fig. 3c), but resulted in a gradually increased inhibition of Cre-mediated activation of the reporter gene in target cells by Nef-defective HIV-1 (Fig. 5c), with a 25-fold inhibition observed at the highest SERINC5 expression level, which in turn inhibited infectivity by 250-fold (Fig. 5c). This observation was reproducible also using a fusion assay based on the viral incorporation and cytoplasmic delivery of a BLAM-VpR chimaeric gene³⁸ (Extended Data Fig. 3d). By contrast, Cre-delivery from Nef-defective HIV-1 pseudotyped with VSV-G (Fig. 5d) or with EBOV GP (Extended Data Fig. 3e) was not inhibited by SERINC5, consistent with the

intrinsic resistance of these pseudotypes to the inhibition by the host factor (Fig. 3b).

When the host factor was expressed at a level which introduced a 20-fold effect on infectivity, SERINC5 resulted in a 2–3-fold inhibition of Cre delivery, fully counteracted by Nef (Extended Data Fig. 3f). Similarly, Nef-defective HIV-1 derived from wild-type JTAG cells delivered Cre to target cells with a 2–3-fold lower efficiency than Nef-positive virions in the presence of endogenously expressed SERINC5, in spite of a 20-fold lower infectivity (Fig. 5e).

Altogether, these results suggest that SERINC5 perturbs the ability of the viral particle to translocate its content to the cytoplasm.

Discussion

Here we demonstrate that SERINC5, and to a lesser extent SERINC3, are responsible for the long-sought anti-HIV-1 activity that is overcome by Nef. These cellular proteins join a growing list of host factors that inhibit retrovirus infection and are referred to as restriction factors. However, SERINC5 and SERINC3 have features that distinguish them from other known retroviral restriction factors. For example, SERINC5 expression in primary CD4⁺ T cells or dendritic cells is not upregulated by type I interferon or by an interferon-inducing agent such as lipopolysaccharide (LPS; Extended Data Fig. 4). SERINC5 and SERINC3 therefore appear to be examples of constitutively expressed intrinsic restriction factors.

Human SERINC5 shares 28% identity at the amino acid level with the *Saccharomyces cerevisiae* orthologue, *TMS1* (ref. 18). Such a degree of conservation suggests a yet unidentified core biological function in cells and represents another peculiar feature compared with other antiretroviral restriction factors (for example, TRIM5 could be traced back only to teleosts³⁹), which diversified under strong positive selection⁴⁰. Remarkably, Nef from HIV-1 and SIV, as well as glycoGag from MLV, are all capable of counteracting human SERINC5, denoting an unusual low species-specificity between the host factor and the viral antagonist.

We provided evidence that SERINC5 perturbs the ability of small intravirion proteins, such as Cre and BLAM-VpR (less than 40 kDa), to access the target cell. However, inhibition of infectivity by SERINC5 is tenfold higher, suggesting that infection is blocked despite detectable fusion. The effect on infectivity, which requires the delivery of the 60–120-nm viral core⁴¹, is therefore unlikely to be explained only by an effect of SERINC5 on the initial membrane fusion event. The host protein could therefore affect a step after the fusion pore generation, required for the translocation of the viral core (Fig. 5f). After the initial membrane fusion triggered by fusogenic glycoproteins, the formation of a fusion pore is followed by its expansion, the highest energy requiring step in the fusion process⁴². This event is known to be affected by the lipid membrane composition^{43,44} and the presence of proteins altering the rigidity and the curvature of the lipid bilayer⁴⁵. How SERINC5 would affect this step of HIV-1 infection remains to be established. By contrast, VSV-G or EBOV GP may override such inhibition by intrinsically promoting more efficient expansion of the fusion pore. Interestingly, some HIV-1 Env glycoproteins from clinical isolates appear also to modulate the susceptibility of the virus to SERINC5 inhibition (Fig. 3c), suggesting the possibility that HIV-1 uses Env in addition to Nef to overcome such a powerful block.

In conclusion, the ability to target evolutionary distant retroviruses (HIV and MLV) and the convergent evolution of antagonistic retroviral factors (Nef and glycoGag) indicate that SERINC5 has a fundamental role in the interaction of the host with retroviral pathogens. Interestingly, ectopic expression of SERINC5 potently inhibits HIV-1, even in the presence of Nef (Fig. 2g), suggesting that this cellular antiviral factor might be exploited as an anti-HIV-1 therapeutic gene.

Online Content Methods, along with any additional Extended Data display items and Source Data, are available in the online version of the paper; references unique to these sections appear only in the online paper.

Received 6 May; accepted 18 August 2015.

Published online 30 September 2015.

1. Kestler, H. W. Importance of the *nef* gene for maintenance of high virus loads and for development of AIDS. *Cell* **65**, 651–662 (1991).
2. Deacon, N. J. et al. Genomic structure of an attenuated quasi species of HIV-1 from a blood transfusion donor and recipients. *Science* **270**, 988–991 (1995).
3. Kirchhoff, F., Greenough, T. C., Brettler, D. B., Sullivan, J. L. & Desrosiers, R. C. Brief report: absence of intact nef sequences in a long-term survivor with nonprogressive HIV-1 infection. *N. Engl. J. Med.* **332**, 228–232 (1995).
4. Landi, A., Iannucci, V., Nuffel, A. V., Meuwissen, P. & Verhasselt, B. One protein to rule them all: modulation of cell surface receptors and molecules by HIV Nef. *Curr. HIV Res.* **9**, 496–504 (2011).
5. Baur, A. S. et al. HIV-1 Nef leads to inhibition or activation of T cells depending on its intracellular localization. *Immunity* **1**, 373–384 (1994).
6. Schrager, J. A. & Marsh, J. W. HIV-1 Nef increases T cell activation in a stimulus-dependent manner. *Proc. Natl Acad. Sci. USA* **96**, 8167–8172 (1999).
7. Alexander, L., Du, Z., Rosenzweig, M., Jung, J. U. & Desrosiers, R. C. A role for natural simian immunodeficiency virus and human immunodeficiency virus type 1 nef alleles in lymphocyte activation. *J. Virol.* **71**, 6094–6099 (1997).
8. Simmons, A., Aluvihare, V. & McMichael, A. Nef triggers a transcriptional program in T cells imitating single-signal T cell activation and inducing HIV virulence mediators. *Immunity* **14**, 763–777 (2001).
9. Stolp, B. et al. HIV-1 Nef interferes with host cell motility by deregulation of Cofilin. *Cell Host Microbe* **6**, 174–186 (2009).
10. Chowers, M. Y. et al. Optimal infectivity *in vitro* of human immunodeficiency virus type 1 requires an intact *nef* gene. *J. Virol.* **68**, 2906–2914 (1994).
11. Munch, J. et al. Nef-mediated enhancement of virion infectivity and stimulation of viral replication are fundamental properties of primate lentiviruses. *J. Virol.* **81**, 13852–13864 (2007).
12. Carl, S. et al. Modulation of different human immunodeficiency virus type 1 Nef functions during progression to AIDS. *J. Virol.* **75**, 3657–3665 (2001).
13. Aiken, C. & Trono, D. Nef stimulates human immunodeficiency virus type 1 proviral DNA synthesis. *J. Virol.* **69**, 5048–5056 (1995).
14. Chowers, M. Y., Pandori, M. W., Spina, C. A., Richman, D. D. & Guatelli, J. C. The growth advantage conferred by HIV-1 nef is determined at the level of viral DNA formation and is independent of CD4 downregulation. *Virology* **212**, 451–457 (1995).
15. Schwartz, O., Marechal, V., Danos, O. & Heard, J. M. Human immunodeficiency virus type 1 Nef increases the efficiency of reverse transcription in the infected cell. *J. Virol.* **69**, 4053–4059 (1995).
16. Pizzato, M. MLV glycosylated-Gag is an infectivity factor that rescues Nef-deficient HIV-1. *Proc. Natl Acad. Sci. USA* **107**, 9364–9369 (2010).
17. Usami, Y., Popov, S. & Gottlinger, H. G. The Nef-Like effect of murine leukemia virus glycosylated Gag on HIV-1 infectivity is mediated by its cytoplasmic domain and depends on the AP-2 adaptor complex. *J. Virol.* **88**, 3443–3454 (2014).
18. Grossman, T. R., Luque, J. M. & Nelson, N. Identification of a ubiquitous family of membrane proteins and their expression in mouse brain. *J. Exp. Biol.* **203**, 447–457 (2000).
19. Xu, J. et al. Cloning and expression of a novel human C5orf12 gene, a member of the TMS_TDE family. *Mol. Biol. Rep.* **30**, 47–52 (2003).
20. Inuzuka, M., Hayakawa, M. & Ingi, T. Serinc, an activity-regulated protein family, incorporates serine into membrane lipid synthesis. *J. Biol. Chem.* **280**, 35776–35783 (2005).
21. Craig, H. M., Pandori, M. W. & Guatelli, J. C. Interaction of HIV-1 Nef with the cellular dileucine-based sorting pathway is required for CD4 down-regulation and optimal viral infectivity. *Proc. Natl Acad. Sci. USA* **95**, 11229–11234 (1998).
22. Pizzato, M. et al. Dynamin 2 is required for the enhancement of HIV-1 infectivity by Nef. *Proc. Natl Acad. Sci. USA* **104**, 6812–6817 (2007).
23. Saksela, K., Cheng, G. & Baltimore, D. Proline-rich (PxxP) motifs in HIV-1 Nef bind to SH3 domains of a subset of Src kinases and are required for the enhanced growth of Nef⁺ viruses but not for down-regulation of CD4. *EMBO J.* **14**, 484–491 (1995).
24. Piguet, V. et al. Nef-induced CD4 degradation: a diacidic-based motif in Nef functions as a lysosomal targeting signal through the binding of β-COP in endosomes. *Cell* **97**, 63–73 (1999).
25. Miller, M. D., Warmerdam, M. T., Page, K. A., Feinberg, M. B. & Greene, W. C. Expression of the human immunodeficiency virus type 1 (HIV-1) *nef* gene during HIV-1 production increases progeny particle infectivity independently of gp160 or viral entry. *J. Virol.* **69**, 579–584 (1995).
26. Aiken, C. Pseudotyping human immunodeficiency virus type 1 (HIV-1) by the glycoprotein of vesicular stomatitis virus targets HIV-1 entry to an endocytic pathway and suppresses both the requirement for Nef and the sensitivity to cyclosporin A. *J. Virol.* **71**, 5871–5877 (1997).
27. Chazal, N., Singer, G., Aiken, C., Hammarskjold, M. L. & Rekosh, D. Human immunodeficiency virus type 1 particles pseudotyped with envelope proteins that fuse at low pH no longer require Nef for optimal infectivity. *J. Virol.* **75**, 4014–4018 (2001).
28. Pizzato, M., Popova, E. & Gottlinger, H. G. Nef can enhance the infectivity of receptor-pseudotyped human immunodeficiency virus type 1 particles. *J. Virol.* **82**, 10811–10819 (2008).
29. Luo, T., Douglas, J. L., Livingston, R. L. & Garcia, J. V. Infectivity enhancement by HIV-1 Nef is dependent on the pathway of virus entry: implications for HIV-based gene transfer systems. *Virology* **241**, 224–233 (1998).
30. Lai, R. P. et al. Nef decreases HIV-1 sensitivity to neutralizing antibodies that target the membrane-proximal external region of TMgp41. *PLoS Pathog.* **7**, e1002442 (2011).
31. Usami, Y. & Gottlinger, H. HIV-1 Nef responsiveness is determined by env variable regions involved in trimer association and correlates with neutralization sensitivity. *Cell Rep.* **5**, 802–812 (2013).
32. Campbell, E. M., Nunez, R. & Hope, T. J. Disruption of the actin cytoskeleton can complement the ability of Nef to enhance human immunodeficiency virus type 1 infectivity. *J. Virol.* **78**, 5745–5755 (2004).
33. Schaeffer, E., Gelezunis, R. & Greene, W. C. Human immunodeficiency virus type 1 Nef functions at the level of virus entry by enhancing cytoplasmic delivery of virions. *J. Virol.* **75**, 2993–3000 (2001).
34. Zhou, J. & Aiken, C. Nef enhances human immunodeficiency virus type 1 infectivity resulting from intervirion fusion: evidence supporting a role for Nef at the virion envelope. *J. Virol.* **75**, 5851–5859 (2001).
35. Tobiume, M., Lineberger, J. E., Lundquist, C. A., Miller, M. D. & Aiken, C. Nef does not affect the efficiency of human immunodeficiency virus type 1 fusion with target cells. *J. Virol.* **77**, 10645–10650 (2003).
36. Cavrois, M., Neidleman, J., Yonemoto, W., Fenard, D. & Greene, W. C. HIV-1 virion fusion assay: uncoating not required and no effect of Nef on fusion. *Virology* **328**, 36–44 (2004).
37. Day, J. R., Munk, C. & Guatelli, J. C. The membrane-proximal tyrosine-based sorting signal of human immunodeficiency virus type 1 gp41 is required for optimal viral infectivity. *J. Virol.* **78**, 1069–1079 (2004).
38. Cavrois, M., De Noronha, C. & Greene, W. C. A sensitive and specific enzyme-based assay detecting HIV-1 virion fusion in primary T lymphocytes. *Nature Biotechnol.* **20**, 1151–1154 (2002).
39. van der Aa, L. M. et al. A large new subset of TRIM genes highly diversified by duplication and positive selection in teleost fish. *BMC Biol.* **7**, 7 (2009).
40. Dugall, N. K. & Emerman, M. Evolutionary conflicts between viruses and restriction factors shape immunity. *Nature Rev. Immunol.* **12**, 687–695 (2012).
41. Briggs, J. A., Wilk, T., Welker, R., Kräusslich, H. G. & Fuller, S. D. Structural organization of authentic, mature HIV-1 virions and cores. *EMBO J.* **22**, 1707–1715 (2003).
42. Cohen, F. S. & Melikyan, G. B. The energetics of membrane fusion from binding, through hemifusion, pore formation, and pore enlargement. *J. Membr. Biol.* **199**, 1–14 (2004).
43. Razinkov, V. I. & Cohen, F. S. Sterols and sphingolipids strongly affect the growth of fusion pores induced by the hemagglutinin of influenza virus. *Biochemistry* **39**, 13462–13468 (2000).
44. Ciechonska, M. & Duncan, R. Lysophosphatidylcholine reversibly arrests pore expansion during syncytium formation mediated by diverse viral fusogens. *J. Virol.* **88**, 6528–6531 (2014).
45. Chen, A. et al. Fusion-pore expansion during syncytium formation is restricted by an actin network. *J. Cell Sci.* **121**, 3619–3628 (2008).

Acknowledgements We thank the Centre for AIDS Reagents, NIBSC, and NIH AIDS Research and Reference Reagent Program, Division of AIDS, for cell lines, plasmids and antibodies. We thank V. Adamo and the CIBIO high-throughput screening and the Advanced Imaging facilities staff for technical assistance, G. De Silvestro, G. Mattiuzzo, C. Reinhard and L. Conti for reagents, G. Melikyan, S. Basmaciogullari, P. Cherepanov, O. Fackler, N. Segata, F. Demichelis, A. Marcello, T. Fedrizzi and A. Helander for critical discussions. This work was supported by the Biotechnology Program of University of Trento, FP7 Marie Curie Career Integration grant number 322130 and Caritro ‘Ricerca Biomedica’ grant number 2013.0248 to M.P., National Institute of Health grant DP1DA034990 to J.L. and European Research Council grant 249968 to S.E.A.

Author Contributions A.R., A.C., S.Z., V.D.S., R.B., S.E.A., J.L., F.A.S. and M.P. designed the experiments. A.R., S.Z., A.C., V.D.S., R.B., S.L.G., S.M.M., A.N., F.A.S. and M.P. performed the experiments. All authors contributed to the assembly and writing of the manuscript. A.R., A.C. and S.Z. contributed equally to the study.

Author Information RNA-seq fastq data have been deposited in NCBI Sequence Read Archive (SRA) under accession code SRP062444. Reprints and permissions information is available at www.nature.com/reprints. The authors declare no competing financial interests. Readers are welcome to comment on the online version of the paper. Correspondence and requests for materials should be addressed to M.P. (massimo.pizzato@unitn.it).

METHODS

Plasmids. Env-defective and nef-defective HIV-1^{NL4-3} have been described previously²². Env-defective and glycoGag-defective MLV were engineered to express GFP in place of Env. Unless otherwise indicated, single round HIV-1 Env-defective HIV-1 (NL4-3) was complemented with Env derived from HIV-1^{HXB2} expressed with the vector PBJ5 (ref. 22). Constructs for expression of other viral factors include: plasmids encoding Env from primary HIV-1 isolates (obtained from NIH AIDS Reagent Program); plasmids encoding wild-type and mutated HA-tagged Nef from HIV-1^{LA1}²² and Nef from primary HIV-1 isolates belonging to subtypes C, D, F; plasmids for expression of HA-tagged Nef from SIV^{mac} and SIV^{agn}²²; plasmids encoding untagged or HA-tagged MLV glycoGag truncated at residue 189 (ref. 16), pCAGGS expressing codon optimized Zaire Ebola virus glycoprotein (GenBank accession number KJ660346.2); pMDG⁴⁶ encoding VSV-G.

DNA encoding SERINC5 with or without the HA-tag were amplified from cDNA derived from JTAG cells. DNA sequence was confirmed to match the reference sequence with accession number NM_001174072.2. DNA encoding SERINC3 (reference sequence NM_006811) was custom synthesized (GeneWiz). For expression in mammalian cells, DNAs were cloned into expression vectors PCDNA3.1 (Life Technologies), PBJ5, PBJ6 (derived from PBJ5 by removing the SV40 origin of replication from the SV40-HTLV-1 hybrid promoter region), and PEGFPN1 (Clontech).

Increasing amount of SERINC5-HA expression in HEK293T cells was obtained by transfecting cells with PBJ6-, PBJ5-, and PCDNA3.1-based vector in increasing order (PBJ6<PBJ5<PCDNA3.1).

mRFP-Rab7 was a gift from A. Helenius (Addgene plasmid 14436). TagRFP657 was fused at the C terminus of Nef to generate pNef-Tag-RFP.

Cell lines. Cell lines used (also described in Extended Data Table 1 together with the source) were all tested for possible contamination with mycoplasma and tested negative. Cell line TE671 (Fig. 1a) is listed in the ICLAC database of commonly misidentified cell lines. However, for our purposes the nature of the cell line does not influence the outcome of the research which was only meant at investigating a correlation between the Nef requirement with gene expression. In addition to cell lines listed in Extended Data Table 1, TZM-bl indicator cells were obtained from the NIH AIDS Research and Reference Reagent program.

CRISPR-Cas9 knockout. Stable cell lines knocked out for SERINC5 were generated by transduction with LentiCRISPR (a gift from F. Zhang, Addgene plasmid 49535) after puromycin selection and, where indicated, clonal expansion. PX330 CRISPR-Cas9 (a gift from F. Zhang, Addgene plasmid 42230) was used for generating knockout by transient transfection, targeting simultaneously two different exons of the same gene. The following target sequences were used: 5'-GC TGAGGGACTGCCGAATCC-3' (SERINC5-1, exon 2), 5'-GACGGCTCCAC ATAGCGCC-3' (SERINC5-2, exon 6), 5'-GGCGTACCAACAGCTTGTAC-3' (SERINC5-3, exon 8), 5'-GCATCGCATAGCAAACAGC-3' and 5'-CTATGC CGATGCTGTCCTAG-3' (SERINC1), 5'-CCGCATCTGCTTCGGCACCG-3' and 5'-ATCCTGGTGGCCTACCGT-3' (SERINC2), 5'-ATAATGAGGC GAGTCACCG-3' and 5'-CTCCGAGCGCAGTACACAA-3' (SERINC3), 5'-TGATGACAGAACGCTTGTAGG-3' and 5'-GGTTCATTACTCAGGC C-3' (SERINC4), 5'-GTGAACCGCATCGAGCTGAA-3' (GFP).

To verify the occurrence of indels and the disruption of the SERINC5 open-reading frame (ORF) in clonal populations of JTAG cells stably transduced with the LentiCRISPR vector targeting SERINC5 exon 2 (using SERINC5-1 gRNA), genomic DNA was extracted from cells, a 228-nucleotide fragment encompassing exon 2 was amplified by PCR using primers 5'-TCGTCGGCAGCGTCAGATG TGTATAAGAGACAG-TAAGCAGATGCCCTCTGTTCTT-3' and 5'-GTCT CGTGGGCTCGGAGATGTGTATAAGAGACAG-AATAGGACGAGCTGAAC ACGG-3' (in which italic denotes the locus-specific sequence, and bold denotes the overhang adaptors). A subsequent limited-cycle amplification step was performed to add multiplexing indices and Illumina sequencing adapters. Normalized and pooled libraries were, then, sequenced on the Illumina MiSeq system using v2 reagents (2×250-nucleotide paired-end reads).

Viruses and infectivity assay. Cell lines in Fig. 1a were infected with NL4-3 and NL4-3^{Nef-} produced by transfection of HEK293T cells and transiently pseudotyped with VSV-G. Virus supernatant was collected 48 h after infection and inoculated onto TZM-bl cells in the presence of the protease inhibitor Saquinavir (10 µM) to limit infection to a single round of replication.

For all other experiments, viruses limited to a single round of replication were used and were produced by transfection. JTAG and 174XCEM cells were transfected using electroporation, HT1080 using Mirus TransIT-2020, HEK293T cells by the calcium phosphate co-precipitation method. PBMC were transfected by nucleofection 48 h after stimulation with phytohaemagglutinin (PHA) and interleukin-2 (IL-2). As indicated, virus constructs were co-transfected together with other plasmids expressing Env glycoproteins, Nef, glycoGag, SERINC5, or PX330-based CRISPR-Cas9 vectors. Virus-containing culture supernatants were

collected 48 h after transfection, clarified by centrifugation at 300g for 5 min and passed through filters with 0.45-µm pores. Virus prepared in quadruplicate were then quantified using the SG-PERT reverse transcription assay⁴⁷, diluted three- or fivefold in a series of six steps and used to infect TZM-GFP reporter cells seeded one day before infection in 96-well plates. TZM-GFP is a modified version of TZM-bl containing an integrated nlsGFP reporter gene under the transcriptional control of the HIV-1 long terminal repeat. Infection of reporter cells was scored using the High Content Imaging System Operetta (Perkin Elmer) after counter-staining nuclei with Hoechst 33342 for each virus dilution. Those values falling into a linear dilution range (normally below 20% of infected cells) were used to calculate infectivity. Infectivity was calculated by dividing the number of infected cells in a well for the amount of reverse transcriptase activity associated to the virus inoculum, measured in mU⁴⁷.

Heterokaryons. Heterokaryons were produced following a strategy previously reported⁴⁸. Production of single round virions infectious only upon heterokaryon formation was obtained by transfecting one fusion partner with env-defective/nef-defective HIV-1^{NL4-3} and the other with PBJ5-HXB2-Env, PBJ5-Nef^{dAl} or the empty control vector PBJ5. To promote efficient fusion mediated by HIV-1 Env, plasmids encoding for CD4 and CXCR4 were co-transfected together with the env-defective provirus construct. Then 24 h after transfection, cells were co-cultured and progeny viruses collected 24 h later.

Preparation of RNA-seq libraries and sequencing. Five micrograms of total RNA extracted from seven highly Nef-dependent cell lines (JTAG, Jurkat E6.1, bl41, Ramos, CEM A301, CEM SS and HSB2) and eight low Nef-dependent cell lines (MT4, HT1080, RAJI, DAUDI, C8166, IMR90, CEMX174 and WI38) was subjected to rRNA depletion using Ribo-Zero Magnetic Gold Kit (Epicentre). RNA-seq libraries were prepared from the rRNA depleted RNAs extracted from the 15 cell lines (Fig. 1a) using a modified protocol of the Illumina TruSeq RNA Sample Prep Kit. Libraries were sequenced on the Illumina HiSeq 2000 using paired-end sequencing 2×100 bp. Raw reads were mapped against the human (hg19) genome reference using tophat2 (ref. 49). RPM⁵⁰ values were estimated for each transcript in each sample with a custom pipeline. Genes were ranked according to Pearson correlation between their relative expression (RPM) in cell line and the corresponding Nef⁺/Nef⁻ infectivity ratio (Fig. 1a). The computations were performed at the Vital-IT Center (<http://www.vital-it.ch>) for high-performance computing of the SIB Swiss Institute of Bioinformatics in Geneva.

Microscopy. JTAG cells were electroporated with constructs expressing Nef-TagRFP657 or the control TagRFP657, Nef-HA, HA-glycoMa, SERINC5-GFP and Rab7-RFP as indicated. Then 48 h after transfection, cells were overlaid on poly-L-lysine coated glass slides, fixed with 4% paraformaldehyde and permeabilized with 0.1% Triton X-100. The HA tag was detected by staining with mouse anti-HA (HA.11, Covance) and the secondary antibody Alexa 633 (Life Technologies). Images were acquired using a Leica TCS SP5 confocal microscope.

Western blotting. Cell lysates and virion pellets were analysed by SDS-PAGE and western blotting. In brief, viral particles were collected 48 h after transfection, centrifuged at 300g to remove cell debris and filtered. The clarified supernatants were overlaid on 25% sucrose cushion and concentrated at 100,000g. The pellets were resuspended directly in Laemmli buffer (supplemented with 50 mM TCEP), normalized by reverse transcriptase assay and resolved by SDS-PAGE. After observing that SERINC5 and SERINC3 form aggregates that are lost while clarifying the cell lysate or fail to enter the separating gel, cells were lysed directly in Laemmli buffer containing TCEP (Sigma, final concentration 50 mM, pH 7.0) and avoiding boiling. Samples were loaded on gel after a 5-pulse sonication. Having failed to find a commercially available antibody capable of detecting the endogenous protein, probing was performed using mouse anti-HA (HA.11, Clone 16B12, Covance), mouse or rabbit anti-β-actin (Li-COR), anti-HIV-1 p55/p24 (National Biological Standards Board), anti-gp41 Chessie-8 (obtained from the NIH AIDS Reagent Program, Division of AIDS, NIAID, NIH from G. Lewis), mouse anti-Cre (Mab3120, Chemicon) and secondary antibodies IRDye 680 and IRDye 800 (Li-COR). Blots were imaged using an Odyssey Imager system (Li-COR).

nlsCre delivery assay. A packaging vector based on p8.9 lentiviral gag-pol expressing plasmid⁴⁶ (8.9-Cre) was generated to carry an insertion of nlsCre between MA and CA flanked by native HIV-protease cleavage sites for processing and release of proteins from Gag.

A Cre-responsive nuclear RFP-expressing lentiviral vector (p-lenti LoxP-Blasti-mRFP) was created. It consists of a nls-mRFP sequence lacking the translation initiation codon and preceded by a sequence encoding the blasticidin antibiotic resistance (Bla) between two loxP sites. The nlsRFP is translationally inactive unless Cre-mediated recombination of loxP and excision of Bla occurs, providing an authentic translation initiation for mRFP. A TZM-bl-GFP derivative cell line (TZM-GFP) stably transduced with p-lenti LoxP-Blasti mRFP was generated (TZM-GFP-LoxP-RFP) to detect delivery of nlsCre, and Tat-driven expression of nlsGFP.

To package nlsCre in retrovirus particles, HIV-1 was produced by mixing 8.9-Cre together with the *env*-defective (and *nef*-defective where applicable) NL4-3 provirus at a ratio of 1:2. Virus was produced by cotransfeting HEK293T cells with the viral constructs together with PBJ5-HXB2-env or vectors for expression of VSV-G and Ebola glycoprotein, and plasmids encoding SERINC5 or the empty vector. To achieve increasing level of expression, SERINC5 was expressed from vector PBJ6, PBJ5 and PCDNA3.1 (in increasing order). Progeny virus was inoculated onto TZM-GFP-LoxP-RFP and red and green fluorescence quantified 48 h later using the High Content Imaging System Operetta (Perkin Elmer) after counterstaining nuclei with Hoechst 33342, following the method described for infectivity.

BLAM-VpR assay. Virus was produced by transfection of HEK293T with the calcium phosphate method in 10 cm tissue culture plates with 10 µg of NL4-3 Envfs/Neffs (bearing a frameshift) together with 2 µg HIV-1 Env expressor, 5 µg of BLAM-VpR vector³⁸ and 5 µg of SERINC5 expression vectors or the empty vector control.

Target cells (TZM-bl) were seeded in clear bottom 96-well plates (Optiplates, Perkin Elmer) at a density of 25,000 cells per well in phenol-Red-free medium one day before assay. Virus samples were normalized for reverse transcriptase activity content and added to wells (200 µl) serially diluted as described for infectivity. Cells were spin-infected for 2 h at 4 °C at 1,550g, virus was removed, cells washed twice with complete medium and incubated for 90 min at 37 °C. Medium was then replaced with GeneBlazer substrate loading solution containing 2 µM CCF2AM (GeneBLAzer *In vivo* Detection Kit, Life Technologies) and 2.5 mM Probenecid (Sigma). Cells were incubated overnight at 11 °C, fixed with 2% paraformaldehyde and plates analysed using the Operetta imaging system for blue and green fluorescence to reveal the number of blue positive cells. Transduction units were derived from the number of blue positive cells divided per reverse transcriptase activity associated to the virus inocula as described for infectivity.

Quantification of HIV-1 reverse transcription products. NL4-3 normalized based on reverse transcriptase activity was incubated with target cells (NP2-CD4-CXCR4). Cell-free virions were normalized by reverse transcriptase activity and incubated with target cells in 6-well plates for 12 h. For each virus, infections were also performed in the presence of 40 µM AZT, to control for contamination of plasmid DNA in the PCR reaction. Cells were collected and washed extensively with PBS. Total DNA was extracted (Qiagen, QIamp DNA mini kit), quantified, and subjected to real-time PCR with a Biorad CFX96 cycler. cDNA was detected with SYBR-Green I based reactions using 100 ng template DNA and 320 nM of each primer pair (5'-ACAAGCTAGTACCAAGTTGAGCCAGATAAG-3' and 5'-GCCGTGCGCGCTTCAGCAAGC-3') in 20 mM Tris-Cl, pH 8.3, 5 mM (NH₄)₂SO₄, 20 mM KCl, 5 mM MgCl₂, 0.1 mg ml⁻¹ BSA, 1/20,000 SYBR Green I (Sigma), and 200 µM dNTPs. The PCR was programmed for 40 cycles of denaturation at 95 °C for 5 s, annealing 55 °C for 5 s, extension at 72 °C for 20 s and acquisition at 80 °C for 5 s. Relative quantification of retroviral cDNA sequences was obtained with respect to standard curves prepared from serial dilutions of DNA derived from the cell culture with the highest infection, diluted in DNA extracted from non-infected cells.

PBMC. Buffy coats obtained from anonymous blood donors were provided by the Department of Immunotransfusion, Padova University Hospital, for experiments involving virus production, or purchased from the New York Blood Center, for interferon induction studies. PBMC were isolated using Ficoll-Paque Plus (GE Healthcare).

Isolation, stimulation and treatment of dendritic cells. CD14⁺ monocytes were enriched from PBMC by positive selection using CD14 MicroBeads following the manufacturer's protocol (Miltenyi Biotec). CD14⁺-enriched cell populations were counted, centrifuged at 200g for 10 min, and resuspended at 2 × 10⁶ cells ml⁻¹ in RPMI-1640 supplemented with 5% human AB+ serum, 1 × MEM non-essential

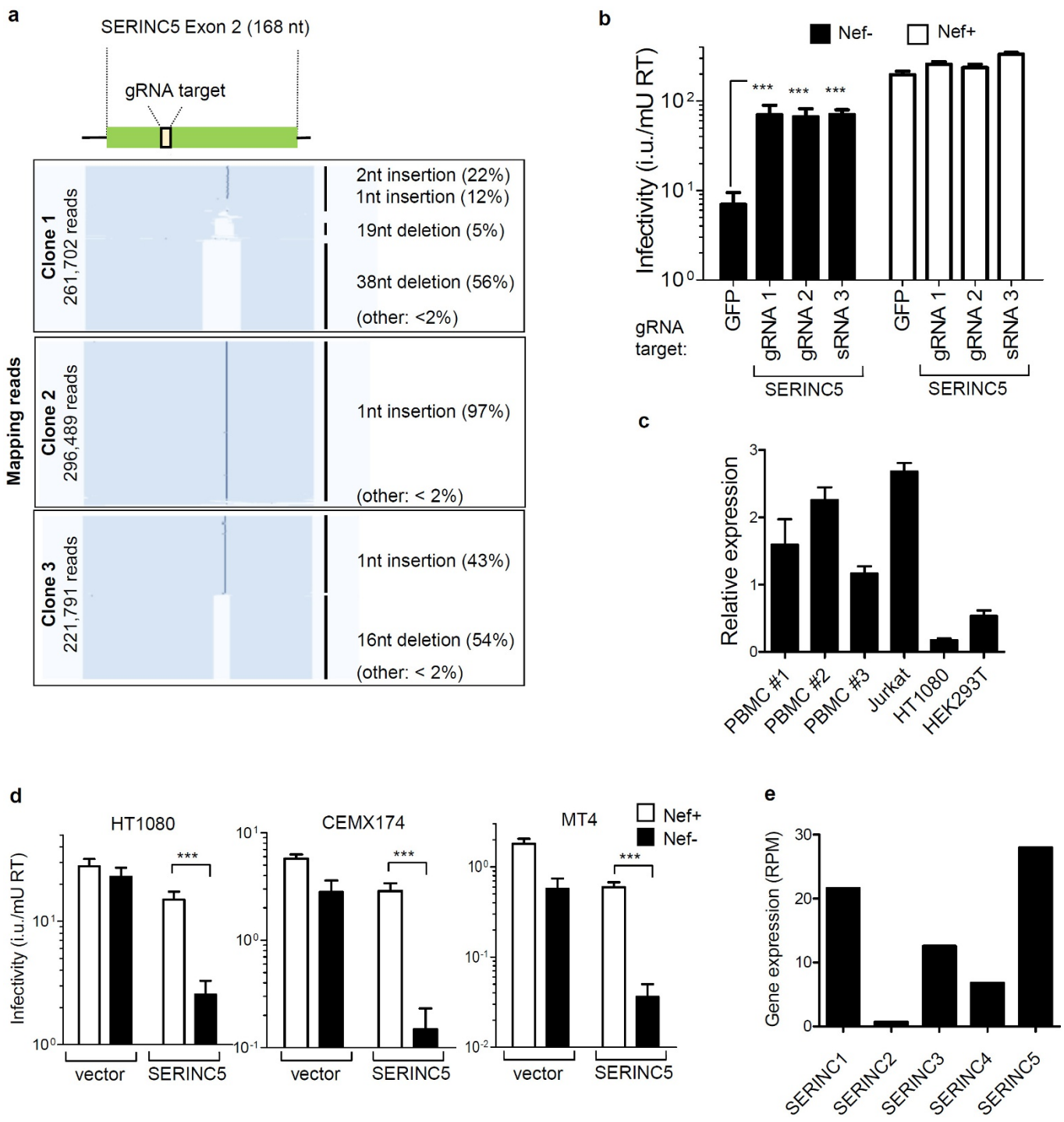
amino acids (NEAA), 20 mM L-glutamine, 25 mM HEPES, 1 mM sodium pyruvate and 50 µM β-mercaptoethanol. To induce differentiation of monocytes into dendritic cells, cells were cultured for 5 days in GM-CSF (50 ng ml⁻¹) and IL-4 (25 ng ml⁻¹), both cytokines from R&D Systems. Dendritic cells were treated with LPS (100 ng ml⁻¹, LPS-EK Ultrapure, Invivogen) or IFN-β (37 ng ml⁻¹, PBL Assay Science). Cells were collected at various time points (*t* = 0 h, 2 h, 6 h, 24 h) after the LPS and IFN-β treatments for RNA extraction and subsequent RT-PCR analysis. **Isolation, stimulation and treatment of CD4⁺ T cells.** CD4⁺ T cells were isolated from CD14-depleted PBMCs by positive selection using CD4 magnetic microbeads (Miltenyi Biotec) and plated at 2 × 10⁶ cells ml⁻¹ in RPMI-1640, supplemented with 10% FBS, 25 mM HEPES, 1 mM sodium pyruvate, 1 × MEM NEAA, and 1 × GlutaMAX (Life Technologies). In one experiment, CD4⁺ T cells were treated directly with LPS (100 ng ml⁻¹) or IFN-β (37 ng ml⁻¹, PBL Assay Science). Separately, CD4⁺ T cells from the same donors were stimulated with 4 µg ml⁻¹ of PHA-M for 48 h, 20 IU ml⁻¹ IL-2 was added, and cells were stimulated with LPS or IFN-β. Cells were collected at various time points (*t* = 0 h, 2 h, 6 h, 24 h) after the LPS and IFN-β treatments for RNA extraction and subsequent RT-PCR analysis. Jurkat T cells were cultured and stimulated similarly. **RNA isolation and qRT-PCR.** RNA was isolated using RNeasy Plus Mini Kit (Qiagen 74134) with additional on column DNase treatment (Qiagen 79254) and reverse transcribed with SuperScript VILO Master Mix (Invitrogen 11755050). Gene expression was assayed on a Biorad CFX96 Real-Time PCR detection system.

For quantification of SERINC5 transcripts in cell lines and PBMC (Extended Data Fig. 2c), the SYBR-Green-based real-time PCR method was used with the following primers 5'-TAAGCAGATGCCTCTGTTCTT-3' and 5'-AATAG GACGAGCTGAACACGG-3' (for SERINC5) and 5'-GACAGGATGCAGAAG GAGATTACTG-3' and 5'-CTCAGGAGGAGCAATGATCTTGAT-3' (for β-actin used as normalization control).

For Extended Data Fig. 4, gene expression was measured using TaqMan Gene Expression Master Mix (Life Technologies 4369016) and the following TaqMan probes and primers sets: SERINC5 (Hs00968169_m1, Life Technologies 4351372) and SERINC3 (Hs01566572_m1), CXCL10 (Hs00171042_m1) and, as a normalization control, OAZ1 (Hs00427923_m1, Life Technologies 4331182).

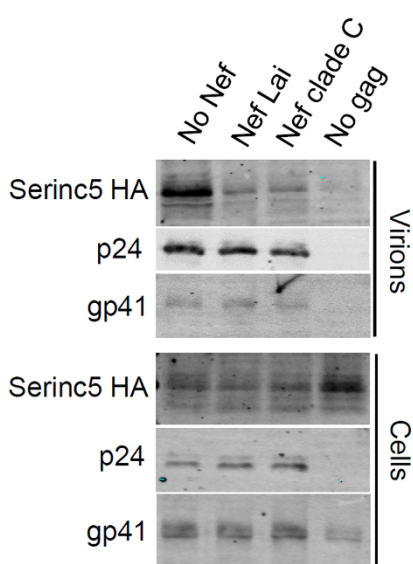
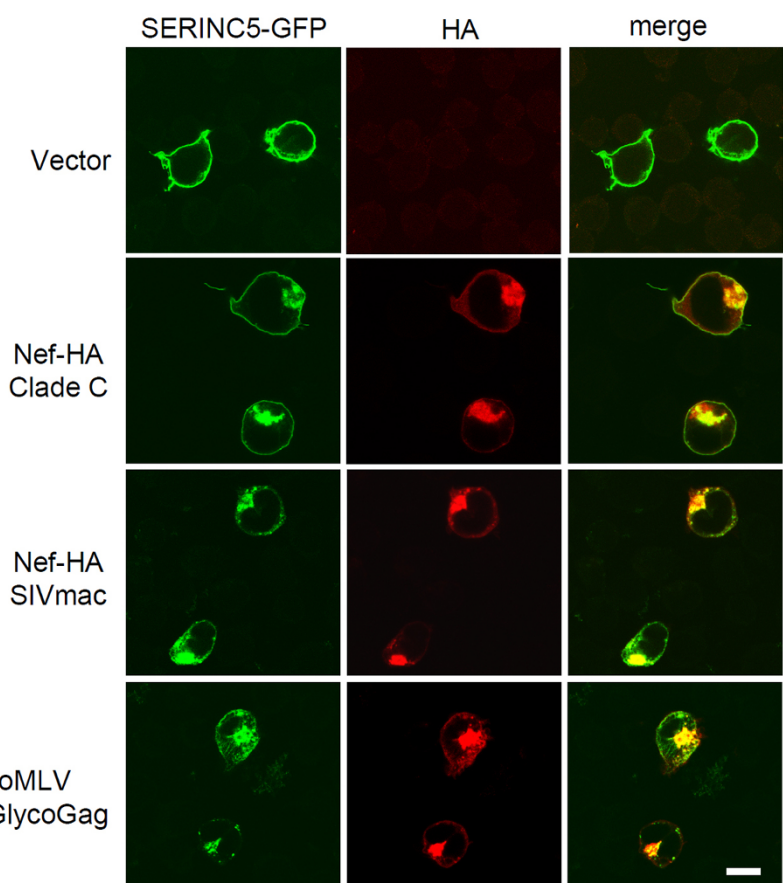
Statistics. Statistical tests were performed using GraphPad Prism. Given the nature of the experiments and the type of samples, significance of differences was assessed with unpaired two-tailed Student's *t*-test. Variance was estimated by calculating the standard deviation in each group, as represented by error bars. Variances between groups of samples were compared using the F-test function integrated in GraphPad. No statistical methods were used to predetermine sample size. Unless otherwise specified in figure legends, all experiments were performed independently at least three times and '*n*' indicates technical replicates, with a representative experiment being shown. Experiments were not randomized, and the investigators were not blinded to allocation during experiments and outcome assessment.

46. Zufferey, R., Nagy, D., Mandel, R. J., Naldini, L. & Trono, D. Multiply attenuated lentiviral vector achieves efficient gene delivery *in vivo*. *Nature Biotechnol.* **15**, 871–875 (1997).
47. Pizzato, M. et al. A one-step SYBR Green I-based product-enhanced reverse transcriptase assay for the quantitation of retroviruses in cell culture supernatants. *J. Virol. Methods* **156**, 1–7 (2009).
48. Simon, J. H., Gaddis, N. C., Fouchier, R. A. & Malim, M. H. Evidence for a newly discovered cellular anti-HIV-1 phenotype. *Nature Med.* **4**, 1397–1400 (1998).
49. Kim, D. et al. TopHat2: accurate alignment of transcriptomes in the presence of insertions, deletions and gene fusions. *Genome Biol.* **14**, R36 (2013).
50. Mortazavi, A., Williams, B. A., McCue, K., Schaeffer, L. & Wold, B. Mapping and quantifying mammalian transcriptomes by RNA-Seq. *Nature Methods* **5**, 621–628 (2008).



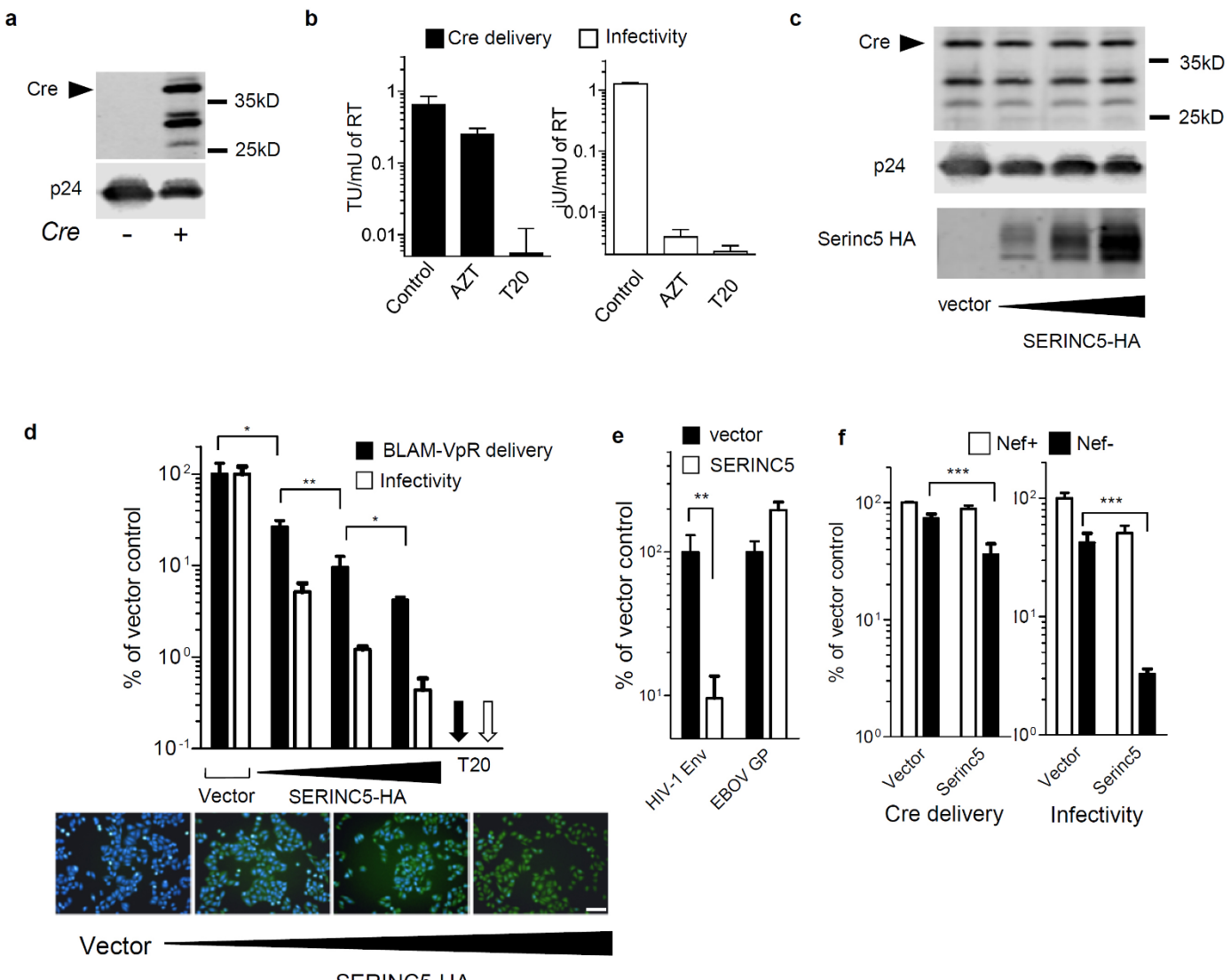
Extended Data Figure 1 | SERINC5 is an inhibitor of HIV-1 infectivity.
a, Mapping of the INDELs in the genomic locus spanning SERINC5 exon 2 in JTAG cell clonal populations from Fig. 2a. **b**, Infectivity of HIV-1 from JTAG cells stably transduced with lentiCRISPR targeting GFP or SERINC5 in three different exons ($n = 4$, experiment replicated twice). **c**, Relative expression of SERINC5 in primary cells and in cell lines measured by qPCR

normalized by expression of *ACTB* ($n = 3$). **d**, Infectivity of HIV-1 from the indicated cell lines expressing SERINC5 ($n = 4$, experiments were replicated twice). Mean \pm s.d., unpaired two-tailed *t*-test, *** $P < 0.001$. **e**, Expression levels of the five SERINC genes in JTAG cells obtained from RNA-seq.

a**b**

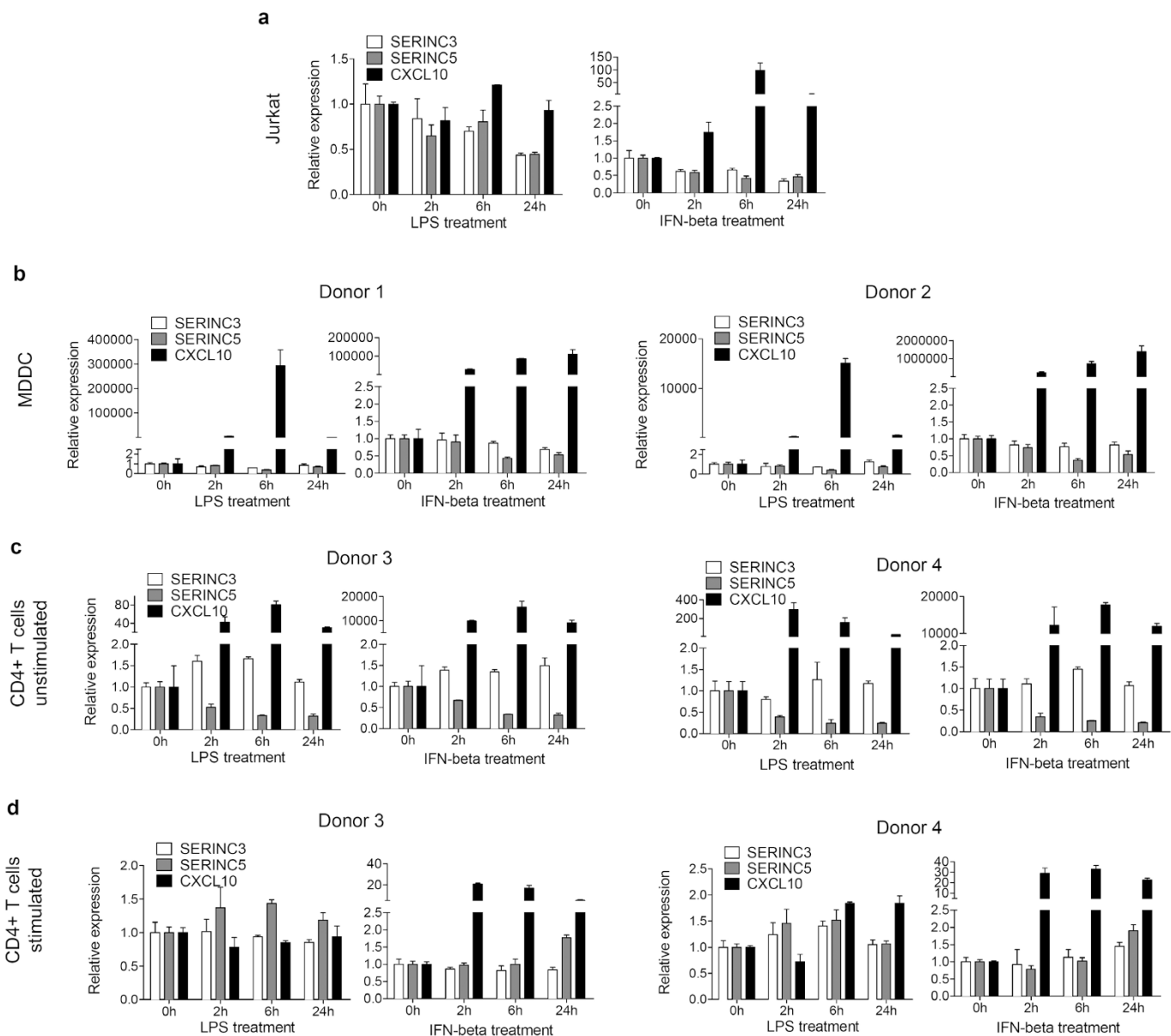
Extended Data Figure 2 | Nef and glycoGag expression result in relocalization of SERINC5 to an endosomal compartment and prevent its incorporation into virions. **a**, Single round Nef-defective NL4-3 produced by cotransfection of HEK293T cells with plasmids expressing Nef proteins or the empty vector control, and PBJ6-SERINC5-HA: immunoblotting of

virions and cell lysates from producer cells. **b**, Immunofluorescence staining of JTAG cells transfected to express SERINC5-GFP, Nef-HA from HIV-1 isolate 97ZA012 (clade C), from SIV^{mac239}, HA-glycoGag or an empty vector control. Scale bar, 10 μ m.



Extended Data Figure 3 | SERINC5 inhibits cytoplasmic delivery of virion content. **a**, Immunodetection of Cre-recombinase (38 kDa) and p24 in HIV-1 particles. **b**, Effect of 1 μ M AZT or 100 nM T20 on Cre-delivery and virus infectivity (TU, transducing units). **c**, Immunoblotting of HIV-1 virus particles produced from HEK293T expressing increasing levels of SERINC5-HA. **d**, Effect of SERINC5 on virus fusion measured with BLAM assay T20 served as

a negative control. ($n = 4$, experiment replicated twice). **e**, Cre delivery by EBOV-GP pseudotyped HIV-1 particles. **f**, Inhibition of Cre delivery and counteraction by Nef on HIV-1 from HEK293T expressing SERINC5. Mean \pm s.d., $n = 4$, unpaired two-tailed t -test, * $P < 0.05$, ** $P < 0.01$, *** $P < 0.001$. Scale bar, 100 μ m.



Extended Data Figure 4 | SERINC3 and SERINC5 expression is not induced by interferon nor LPS treatments. **a–d**, Relative gene expression levels of SERINC3, SERINC5 and CXCL10 in response to treatment with IFN- β and LPS in Jurkat (a), monocyte-derived dendritic cells from two donors (MDDC, b),

CD4 $^{+}$ primary T cells unstimulated (c) or stimulated with PHA (d) from two donors. Expression of the housekeeping gene OAZ1 was used as a normalization control. Mean \pm s.d., $n = 3$.

Extended Data Table 1 | Description of the cells lines used in Fig. 1a

Cell Line	Cell Type	Source
Jurkat E6.1	T Lymphocyte, Acute T Cell Leukemia	ATCC
Jurkat TAg	T Lymphocyte, Acute T Cell Leukemia. Derivative of Jurkat E6.1, contains SV40 LargeT antigen	Heinrich Gottlinger, DFCI, Harvard University
bl41	B-Lymphocyte, Burkitt's lymphoma	Paul Farrell, Imperial College London
Ramos	B-Lymphocyte, Burkitt's lymphoma	ATCC
CEM-CCRF	T-Lymphocyte, Acute Lymphoblastic Leukemia	ATCC
CEM/A3.01	T-Lymphocyte, Acute Lymphoblastic Leukemia Derivative of CEM-CCRF	NIH AIDS Reagent Program
CEMSS	T-Lymphocyte, Acute Lymphoblastic Leukemia.	NIH AIDS Reagent Program
HSB-2	T-Lymphocyte, Acute Lymphoblastic Leukemia, CD4-	NIH AIDS Reagent Program
H9	T-Lymphocyte, human cutaneous T cell lymphoma. Derivative of HUT-78	NIH AIDS Reagent Program
DG7 HAD	B-Lymphocyte, Burkitt's lymphoma	Sidney Grossberg, University of Wisconsin
HeLa	Epithelial, cervix adenocarcinoma	ATCC
Akata	B-Lymphocyte, Burkitt's lymphoma	Paul Farrell, Imperial College London
SupT1	T-Lymphocyte, T-Cell Lymphoblastic Lymphoma	NIH AIDS Reagent Program
A549	Epithelial, lung carcinoma	ATCC
HepG2	Hepatocellular Carcinoma	ATCC
HCT116	Epithelial, colorectal carcinoma	ATCC
MCF7	Epithelial, adenocarcinoma	ATCC
HUT78	T-Lymphocyte, human cutaneous T cell lymphoma	NIH AIDS Reagent Program
293T	Epithelial, embryonic Kidney	ECACC
MT2	T Lymphocyte, T-cell leukemia	NIH AIDS Reagent Program
TE671	Rhabdomyosarcoma	Yasuhiro Takeuchi, UCL, London
Huh-7	Hepatocellular Carcinoma	Michel Strubin, University of Geneva
LL24	Lung Fibroblast	ATCC
RAJI	B-Lymphocyte, Burkitt's lymphoma	ATCC
C8166	T lymphocytes, T cell leukaemia	NIH AIDS Reagent Program
WI38	Lung fibroblast	ATCC
Daudi	B-Lymphocyte, Burkitt's lymphoma	Paul Farrell, Imperial College London
MT4	T lymphocytes, T cell leukaemia	NIH AIDS Reagent Program
IMR-90	Lung fibroblast	ATCC
CEMX174	Lymphocytes, Fusion between a B cell line and a human T cell line	NIH AIDS Reagent Program
HT1080	Epithelial, fibrosarcoma	Yasuhiro Takeuchi, UCL, London